Contribution from the Departments of Chemistry, University of Denver, Denver, Colorado 80208, and University of Colorado at Denver, Denver, Colorado 80202

Metal–Nitroxyl Interactions. 24. Electron Spin Delocalization in Vanadyl and Copper(II) Bis(β-diketonates)

BHIMRAO M. SAWANT,† A. LAURIE W. SHROYER, GARETH R. EATON,* and SANDRA S. EATON*

Received July 13, 1981

Electron–electron spin–spin interaction has been observed in the room temperature solution EPR spectra of a series of spin-labeled pyridines coordinated to vanadyl bis(trifluoroacetylacetonate), vanadyl bis(hexafluoroacetylacetonate), and copper bis(hexafluoroacetylacetonate). In the vanadyl complexes, the spin–spin coupling constant, J, is greater when the spin label is attached to the 4-position of the pyridine ring than when it is attached to the 3-position of the ring. Two isomers exist for the copper complexes of some of the 3-substituted ligands, but for comparable geometries of the adducts the spin–spin coupling is about as large for the 4-substituted ligands as for the 3-substituted ligands. Variation of the linkage between the pyridine ring and the nitroxyl ring results in changes in spin–spin interaction such that J increases in the order ester < amide < Schiff base linkages. The nitroxyl ring influences the magnitude of J such that J increases in the order piperidine < pyrrolidine < pyrroline ~ tetrahydropyridine.

Introduction

We have previously reported that electron–electron spin–spin interaction results in resolved AB splitting patterns in the room-temperature solution EPR spectra of spin-labeled copper(II) and silver(II) complexes.[1-3] For spectra of species dissolved in low viscosity solvents, dipolar interactions between the two unpaired electrons are expected to be largely averaged out by molecular tumbling and the observed coupling is attributed to electron–electron exchange.[1] Thus the spin–spin coupling constant, J, depends on the extent of delocalization of the metal and nitroxyl unpaired electrons, and changes in J, within a series of compounds, can provide information concerning changes in electron delocalization due to changes in metal ion,[3] conformational effects,[4,5] and weak orbital interactions.[6]

In this paper we report the first examples of resolved AB splitting in the EPR spectra of spin-labeled vanadyl complexes. We have analyzed the solution EPR spectra of the spin-labeled pyridines I–XI coordinated to vanadyl bis(hexafluoroacetylacetonate), $VO(hfac)_2$, vanadyl bis(trifluoroacetylacetonate), $VO(tfac)_2$, and copper bis(hexafluoroacetylacetonate), $Cu(hfac)_2$. The series of ligands was chosen to permit comparison of spin delocalization (1) through the 3- and 4-positions of a pyridine ring coordinated to VO^{2+} and Cu^{2+}, (2) through ester, amide, and Schiff base linkages between the pyridine and nitroxyl rings, and (3) through 5- and 6-membered nitroxyl rings with and without a double bond in the nitroxyl ring.

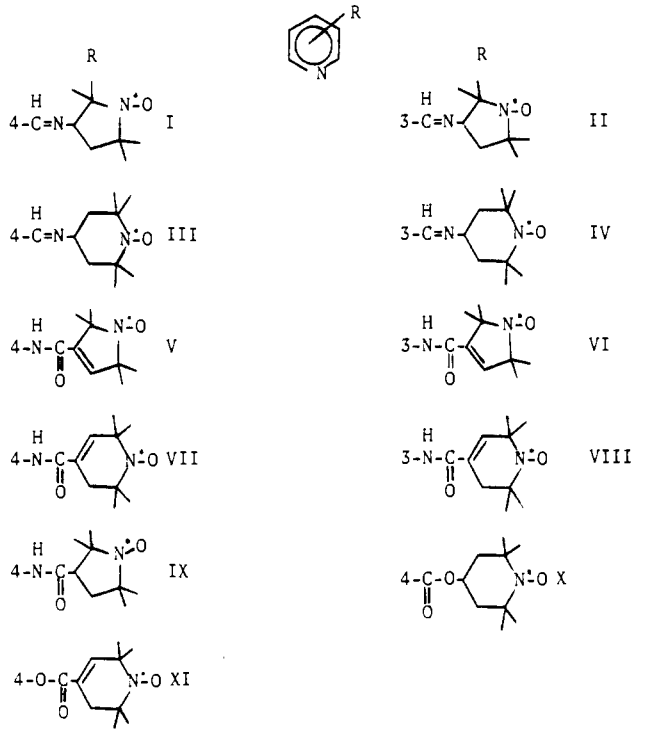

Experimental Section

Physical Measurements. Infrared spectra were obtained on a Perkin-Elmer 337 grating spectrometer using halocarbon or Nujol mulls or in CH_2Cl_2 solution. Electronic spectra were recorded on a Beckman Acta V spectrometer. X-band EPR spectra were obtained on a Varian E-9 spectrometer[7] using deoxygenated solutions. Q-band EPR spectra were obtained as previously described.[8] Solution concentrations were (1–3) × 10^{-3} M. g values were measured relative to DPPH (2.0036). All coupling constants are given in gauss (1 gauss = 0.1 mT) to facilitate comparison with the field-swept experimental spectra. Elemental analyses were performed by Spang Microanalytical Laboratory.

Preparation of Compounds. All starting materials were commercially available and were used as received unless specified otherwise. The following compounds were prepared by literature methods: $Cu(hfac)_2$,[9] $VO(tfac)_2$,[10] $VO(hfac)_2$,[11] I,[12] II,[12] III,[13] and IV.[13]

4-[(((2,2,5,5-Tetramethyl-1-oxypyrrolin-3-yl)carbonyl)amino)]-pyridine (V). The acid chloride prepared from 2,2,5,5-tetramethyl-1-oxypyrrolinyl-3-carboxylic acid[14] (1.10 g) was treated with dry THF (75 mL), pyridine (2 mL), and 4-aminopyridine (0.450 g). The reaction mixture was refluxed overnight and the solvent removed in vacuum. The residue was dissolved in $CHCl_3$ (75 mL), washed

* To whom correspondence should be addressed: G.R.E., University of Denver; S.S.E., University of Colorado at Denver.
† On sabbatical leave, 1979–1981, from the Department of Chemistry, Shivaji University, Kolhapur, India.

(1) Eaton, G. R.; Eaton, S. S. *Coord. Chem. Rev.* **1978**, *26*, 207–62.
(2) Eaton, S. S.; DuBois, D. L.; Eaton, G. R. *J. Magn. Reson.* **1978**, *32*, 251–63.
(3) More, K. M.; Eaton, S. S.; Eaton, G. R. *J. Am. Chem. Soc.* **1981**, *103*, 1087–90 and references therein.
(4) Sawant, B. M.; Braden, G. A.; Smith, R. E.; Eaton, G. R.; Eaton, S. S. *Inorg. Chem.* **1981**, *20*, 3349–54.
(5) More, K. M.; Eaton, S. S.; Eaton, G. R. *Inorg. Chem.* **1981**, *20*, 2641–7.
(6) More, K. M.; Sawant, B. M.; Eaton, G. R.; Eaton, S. S. *Inorg. Chem.*, **1981**, *20*, 3354–62.
(7) DuBois, D. L.; Eaton, G. R.; Eaton, S. S. *J. Am. Chem. Soc.* **1978**, *100*, 2686–9.
(8) Eaton, S. S.; More, K. M.; DuBois, D. L.; Boymel, P. M.; Eaton, G. R. *J. Magn. Reson.* **1980**, *41*, 150–7.
(9) Funck, L. L.; Ortolano, T. R. *Inorg. Chem.* **1968**, *7*, 567–73.
(10) Rowe, R. A.; Jones, M. M. *Inorg. Synth.* **1957**, *5*, 113–6.
(11) Su, C.; Reed, J. W.; Gould, E. S. *Inorg. Chem.* **1973**, *12*, 337–43. Drago, R. S.; Kuechler, T. C.; Kroeger, M. *Ibid.* **1979**, *18*, 2337–42.
(12) Boymel, P. M.; Eaton, G. R.; Eaton, S. S. *Inorg. Chem.* **1980**, *19*, 727–35.
(13) Boymel, P. M.; Braden, G. A.; Eaton, G. R.; Eaton, S. S. *Inorg. Chem.* **1980**, *19*, 735–9.
(14) Rozantsev, E. G. "Free Nitroxyl Radicals"; translated by B. J. Hazzard; Plenum Press: New York, 1970; p 209.

0020-1669/82/1321-1093$01.25/0

repeatedly with 0.1 NaOH (total volume ca. 200 mL), washed once with water, and dried over anhydrous Na_2SO_4. The solvent was removed in vacuo. The residue was dissolved in a minimum volume of $CHCl_3$. The solution was put on an alumina column (Baker 0537, activity III, 150 g). The product eluted with $CHCl_3$ as a slow-moving yellow band and was recrystallized from CH_2Cl_2/Et_2O; yield 45%, mp 155 °C. IR: $\nu_{C=C}$ 1595, $\nu_{C=O}$ 1675, ν_{NH} 3220 cm^{-1} (br). EPR ($CHCl_3$): $g = 2.0057$, $A_N = 14.6$ G. Anal. Calcd for $C_{14}H_{18}N_3O_2$: C, 64.60; H, 6.97; N, 16.14. Found: C, 64.52; H, 6.79; N, 15.93.

3-[(((2,2,5,5-Tetramethyl-1-oxypyrrolin-3-yl)carbonyl)amino)]pyridine (VI). The amide was prepared from the acid chloride of 2,2,5,5-tetramethyl-1-oxypyrrolinyl-3-carboxylic acid and 3-aminopyridine with use of the procedure reported for V; yield 45%, mp 151–152 °C. IR: $\nu_{C=C}$ 1590, $\nu_{C=O}$ 1670, ν_{NH} 3150, 3220 cm^{-1}. EPR ($CHCl_3$): $g = 2.0057$, $A_N = 14.6$ G. Anal. Calcd for $C_{14}H_{18}N_3O_2$: C, 64.60; H, 6.97; N, 16.14. Found: C, 64.66; H, 6.86; N, 16.23.

4-[(((2,2,6,6-Tetramethyl-1-oxy-1,2,5,6-tetrahydropyridin-4-yl)carbonyl)amino)]pyridine (VII). The amide was prepared from the acid chloride of 2,2,6,6-tetramethyl-1-oxy-1,2,5,6-tetrahydropyridinyl-4-carboxylic acid[15] and 4-aminopyridine with the procedure reported for V; yield 25%, mp 184–185 C. IR: $\nu_{C=C}$ 1595, $\nu_{C=O}$ 1680, ν_{NH} 3240 cm^{-1}. EPR ($CHCl_3$): $g = 2.0057$, $A_N = 15.3$ G. Anal. Calcd for $C_{15}H_{20}N_3O_2$: C, 65.67; H, 7.35; N, 15.32. Found: C, 65.54; H, 7.33; N, 15.12.

3-[(((2,2,6,6-Tetramethyl-1-oxy-1,2,5,6-tetrahydropyridin-4-yl)carbonyl)amino)]pyridine (VIII). The amide was prepared from the acid chloride of 2,2,6,6-tetramethyl-1-oxy-1,2,5,6-tetrahydropyridinyl-4-carboxylic acid[15] and 3-aminopyridine with the procedure reported for V; yield 42%, mp 181 °C. IR: $\nu_{C=C}$ 1595, $\nu_{C=O}$ 1680, ν_{NH} 3300 cm^{-1} (br). EPR ($CHCl_3$): $g = 2.0057$, $A_N = 15.3$ G. Anal. Calcd for $C_{15}H_{20}N_3O_2$: C, 65.67; H, 7.35; N, 15.32. Found: C, 65.67; H, 7.32; N, 15.27.

4-[(((2,2,5,5-Tetramethyl-1-oxypyrrolidin-3-yl)carbonyl)amino)]pyridine (IX). The amide was prepared from the acid chloride of 2,2,5,5-tetramethyl-1-oxypyrrolidinyl-3-carboxylic acid and 4-aminopyridine with the procedure reported for V; yield 15%, mp 145 °C. IR: $\nu_{C=C}$ 1590, $\nu_{C=O}$ 1705, ν_{NH} 3280 cm^{-1}. EPR ($CHCl_3$): $g = 2.0056$, $A_N = 14.5$ G. Anal. Calcd for $C_{14}H_{20}N_3O_2$: C, 64.10; H, 7.69; N, 16.02. Found: C, 63.84; H, 7.68; N, 16.08.

4-[(((2,2,6,6-Tetramethyl-1-oxypiperidin-4-yl)oxy)carbonyl)]pyridine (X). Isonicotinyl chloride was prepared by refluxing isonicotinic acid (4.0 g) and thionyl chloride (40 mL) for 3 days.[16] Excess thionyl chloride was removed under vacuum, and the residue was dried in vacuo at room temperature for 4 h. The residue was treated with dry THF (75 mL), dry pyridine (2 mL), and 4-hydroxy-2,2,6,6-tetramethyl-1-oxypiperidine (1.0 g). The reaction mixture was refluxed overnight and the solvent removed under vacuum. The crude product was dissolved in $CHCl_3$ and chromatographed on silica gel. The product eluted with $CHCl_3$ as a rapidly-moving orange band. The product was sublimed at ~72 °C (~0.1 mm pressure); yield 65%, mp 82 °C. IR: $\nu_{C=O}$ 1730 cm^{-1}. EPR ($CHCl_3$): $g = 2.0059$, $A_N = 15.7$ G. Anal. Calcd for $C_{15}H_{21}N_2O_3$: C, 64.96; H, 7.63; N, 10.10. Found: 64.94; H, 7.56; N, 10.03.

4-[(((2,2,6,6-Tetramethyl-1-oxy-1,2,5,6-tetrahydropyridin-4-yl)carbonyl)oxy)]pyridine (XI). The ester was prepared from the acid chloride of 2,2,6,6-tetramethyl-1-oxy-1,2,5,6-tetrahydropyridinyl-4-carboxylic acid and 4-hydroxypyridine with the procedure reported for V except that silica gel was used for the chromatography and the product was recrystallized from CH_2Cl_2/petroleum ether (40–60 °C). Final purification was by sublimation at 75 °C (0.1 mm pressure); yield 30%, mp 98–99 °C. IR: $\nu_{C=C}$ 1590, $\nu_{C=O}$ 1740 cm^{-1}. EPR ($CHCl_3$): $g = 2.0058$, $A_N = 15.3$ G. Anal. Calcd for $C_{15}H_{19}N_2O_3$: C, 65.44; H, 6.96; N, 10.17. Found: C, 65.20; H, 6.74; N, 9.88.

Computer Simulations

A slightly modified version of the computer program CUNO[2] was used to simulate the EPR spectra. The Hamiltonian used in the program is given in eq 1, where g_1 and g_2 are the g values of the metal and nitroxyl electrons, $\hat{S}_1$ and $\hat{S}_2$, refer to the metal and nitroxyl electron spins, respectively, J is the electron–electron coupling constant in hertz, I_1, I_2, and I_3 refer to the

$$\mathcal{H} = g_1\beta H\hat{S}_{1Z} + g_2\beta H\hat{S}_{2Z} + hJ\hat{S}_{1Z}\hat{S}_{2Z} + (hJ/2)(\hat{S}_{1+}\hat{S}_{2-} + \hat{S}_{1-}\hat{S}_{2+}) + hA_M\hat{S}_{1Z}\hat{I}_{1Z} + hA_N\hat{S}_{1Z}\hat{I}_{2Z} + hA_{N'}\hat{S}_{2Z}\hat{I}_{3Z} + (hA_M/2)(\hat{S}_{1+}\hat{I}_{1-} + \hat{S}_{1-}\hat{I}_{1+}) - g_M\beta_N H\hat{I}_{1Z} - g_N\beta_N H\hat{I}_{2Z} - g_{N'}\beta_N H\hat{I}_{3Z} \quad (1)$$

metal nuclear spin, the nuclear spin of the coordinated nitrogens, and the nuclear spin of the nitroxyl nitrogen, respectively, A_M is the metal electron–metal nuclear coupling constant in hertz, A_N is the coupling constant in hertz between the metal electron and the nuclear spins of the coordinated nitrogens, $A_{N'}$ is the coupling constant in hertz between the nitroxyl electron and the nuclear spin of the nitroxyl nitrogen, and all other symbols are defined as in ref 2. The first seven terms in the Hamiltonian were treated exactly, and the last four were treated as a perturbation to second order for the transition energies and to first order for the transition probabilities. As originally described,[2] the program was written for metal ions with $S = {}^1/_2$ and $I = {}^3/_2$. The program has subsequently been revised to calculate spectra for any metal ion with $S = {}^1/_2$. In the original program[2] it was assumed that line widths varied as $A + Bm_I + Cm_I^2$, where m_I is the metal nuclear spin state. When J is small, this approach appears to work well. However, as J becomes large other factors contribute to the line width. The program has therefore been modified to permit, when desired, input of numerical values for line widths of individual lines in the spectrum.

So that visual comparison with the field-swept experimental spectra could be facilitated, the values of J, A_M, A_N, and $A_{N'}$ are discussed below in units of gauss with the conversion between hertz and gauss given by eq 2–4. The conversion factor for A_N is the same as for A_M. Only the absolute value of J can be determined from these experiments.

$$J\ (\mathrm{G}) = [J\ (\mathrm{Hz})]\frac{h}{2\beta}\left(\frac{1}{g_1} + \frac{1}{g_2}\right) \quad (2)$$

$$A_M\ (\mathrm{G}) = [A_M\ (\mathrm{Hz})]\frac{h}{g_1\beta} \quad (3)$$

$$A_{N'}\ (\mathrm{G}) = [A_{N'}\ (\mathrm{Hz})]\frac{h}{g_2\beta} \quad (4)$$

The electron–electron coupling results in AB patterns in the EPR spectra. The lines in the spectra are referred to as metal or nitroxyl depending on the nature of the transitions as $J \rightarrow 0$. When J is small relative to the g-value difference between the metal and nitroxyl electrons, each of the metal and nitroxyl lines is split into a doublet. As J becomes larger, the intensity of the outer lines of the AB pattern goes to 0 and the positions of the inner metal and inner nitroxyl lines become equal.

The EPR parameters for $VO(tfac)_2$·py ($g = 1.968 \pm 0.001$, $A_V = 107.0 \pm 0.5$ G), $VO(hfac)_2$·py ($g = 1.968 \pm 0.001$, $A_V = 108.0 \pm 0.5$ G), and $Cu(hfac)_2$·py ($g = 2.149 \pm 0.001$, $A_{Cu} = 52.0 \pm 1.0$ G) were used as starting parameters in the simulations of the spectra of the analogous complexes with paramagnetic ligands. Best fit to the spectra in all cases required changes of 1.0 G or less in A_M and 0.001 or less in the g value. The nitroxyl parameters were $g = 2.0059 \pm 0.0002$ and $A_N = 14.5$–15.7 depending on the size of the nitroxyl ring and the solvent.

Results and Discussion

EPR Spectra of the Vanadyl Complexes. The room-temperature EPR spectrum of $VO(hfac)_2$·py in solution is an eight-line pattern due to coupling between the unpaired electron and the spin-${}^7/_2$ vanadyl nucleus. When spin-labeled ligand IV coordinates to $VO(hfac)_2$ in CH_2Cl_2 solution, the EPR spectra shown in Figure 1 are obtained. The solution contained a 1:1.2 ratio of $VO(hfac)_2$ to ligand IV to shift the equilibrium of (5) toward complex formation. Excess IV

$$VO(hfac)_2 + L \rightleftharpoons VO(hfac)_2{\cdot}L \quad (5)$$

(15) Wong, L. T. L.; Schwenk, R.; Hsia, J. C. *Can. J. Chem.* **1974**, *52*, 3381–3.
(16) Meyer, H.; Graf, R. *Ber. Dtsch. Chem. Ges.* **1928**, *61*, 2202–15.

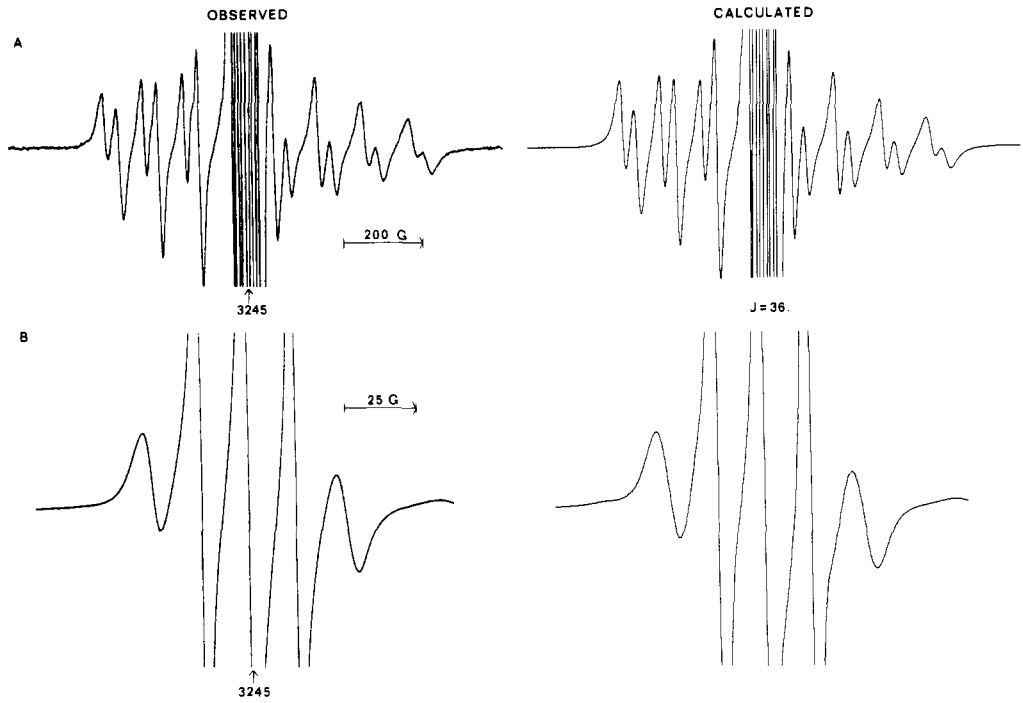

Figure 1. X-band EPR spectra of $VO(hfac)_2$·IV in CH_2Cl_2 solution at room temperature and computer simulations: (A) 1200-G scan obtained with 60-mW power and 0.8-G modulation amplitude; (B) 150-G scan obtained with 15-mW power and 0.5-G modulation amplitude.

interferes to a lesser extent with the spectrum of $VO(hfac)_2$·IV than does $VO(hfac)_2$. The g value of the nitroxyl electron (2.0059) is larger than for the vanadyl electron (1.968) so at X-band the nitroxyl triplet occurs slightly to low field from the center of the vanadyl eight-line pattern. Each of the eight lines in the vanadyl spectrum is split into a doublet due to coupling with the nitroxyl electron. One doublet of vanadyl lines is obscured by the sharper nitroxyl lines. The spacings within the doublets are equal to J which is 36 G for this complex. The nitroxyl signals are also split into doublets due to interaction with the vanadyl electron. The doublet of triplets is partially obscured by the sharper lines from free IV. Addition of excess $VO(hfac)_2$ to the solution causes formation of dimers in which the pyridine nitrogen of IV coordinates to $VO(hfac)_2$ and the nitroxyl oxygen coordinates to a second $VO(hfac)_2$. When the nitroxyl oxygen coordinates to $VO(hfac)_2$, no EPR signal is observed for the nitroxyl or vanadyl electrons.

The room-temperature EPR spectrum of $VO(hfac)_2$·VII in CH_2Cl_2 solution is shown in Figure 2. The spectrum was obtained with a 1:1 ratio of $VO(hfac)_2$ to ligand VII. Computer simulations indicated that the solution contains 94% $VO(hfac)_2$·VII and 6% each of free $VO(hfac)_2$ and free ligand VII. The positions of the signals due to free $VO(hfac)_2$ are marked below the spectrum. The assignments of the lines are based on the assumption that A_V is negative,[17] but the analysis of the spectrum does not depend on this assumption. The sharp three-line pattern centered at 3245 G is due to free ligand VII. The simulated spectrum was obtained with J = 425 G. This value of J is sufficiently large that there is substantial overlap of the vanadyl and nitroxyl lines. For example, interaction of the vanadyl spin −3.5 line with the nitroxyl spin 0 line results in a metal outer line at 2600 G, a metal inner line at 3027 G, a nitroxyl inner line at 3138 G, and a nitroxyl outer line at 3561 G while interaction of the vanadyl spin −1.5 line with the nitroxyl spin 0 line results in a metal outer line at 2746 G, a metal inner line at 3171 G, a nitroxyl inner line at 3191 G, and a nitroxyl outer line as 3614 G. Since the spectrum was obtained with variable magnetic field and fixed frequency, the spacings between inner and outer lines differ slightly from the value of J.[2] The assignments of all the lines are given below the calculated spectrum. The nitroxyl lines are labeled with the nuclear spin state of the vanadyl to which they are coupled. Since the nitrogen hyperfine splitting of the nitroxyl lines is well resolved in the experimental spectrum, it is included in the assignment scheme. The splitting of the metal lines by the nitroxyl nitrogen spin is much smaller and was not included in the schematic although it was included in the simulations. The patterns centered at 2650 and 3850 G are due to the vanadyl outer lines. The lowest and highest field outer lines have greater intensity than the other outer lines because the energy separation between the ±3.5 vanadyl lines and the nitroxyl lines are greater than for the other vanadyl spin states. For the vanadyl ±0.5 spin states, the separation between the vanadyl and nitroxyl signals is so small that the intensity of the outer lines in the AB patterns is negligible. The outer nitroxyl lines are obscured by the ±3.5 lines of free $VO(hfac)_2$.

When ligand VII coordinates to $VO(tfac)_2$ instead of $VO(hfac)_2$, the EPR spectrum shown in Figure 3A is obtained. Although the lines in the spectrum occur at about the same field positions as in Figure 2A, the patterns are more complicated. The low-field outer lines centered at 2650 G give an apparent four-line pattern instead of three lines, and the intensities do not decrease toward high field as observed in Figure 2A. At high field there are six outer lines instead of three lines. The center portion of the spectrum is also more complicated than in Figure 2A. The simulated spectrum was obtained with equal populations of two species with values of J equal to 375 and 435 G. The nature of the two species is discussed below.

The Q-band EPR spectrum of $VO(hfac)_2$·I in CH_2Cl_2 solution is shown in Figure 4. At this frequency the nitroxyl signals occur close to the vanadyl spin −2.5 line. The positions of the lines for free $VO(hfac)_2$ and for $VO(hfac)_2$·L are marked below the spectrum. The nitroxyl lines are labeled with the nuclear spin of the vanadyl to which they are coupled. Nitrogen hyperfine splitting was included in the simulation but was not included in the assignment schematic. The simulated spectrum was obtained with J = 2000 G. This value

(17) Wilson, R.; Kivelson, D. *J. Chem. Phys.* **1966**, *44*, 154–68.

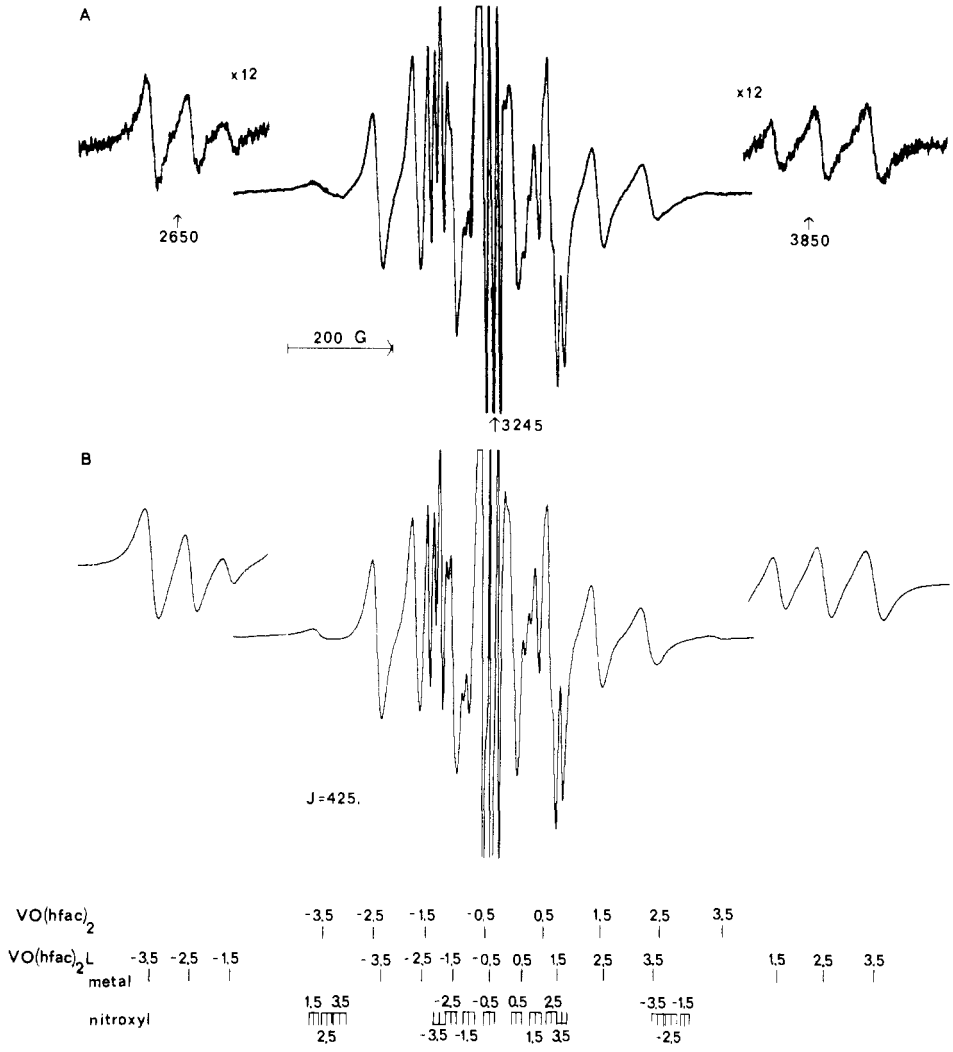

Figure 2. X-band EPR spectra of $VO(hfac)_2$·VII in CH_2Cl_2 solution at room temperature. (A) 1000-G scan of the inner lines of the AB pattern obtained with 40-mW power and 1.0-G modulation amplitude. The inserts show the metal outer lines of the AB patterns and were obtained with the product of modulation amplitude, gain, and square root of power 12 times greater than for the center lines of the spectrum. (B) Computer-simulated spectrum obtained with J = 425 G. The assignments of the lines are given below the spectrum; see text for details.

of J is sufficiently large that for several of the vanadyl spin states the vanadyl and nitroxyl inner lines are nearly coincident. Due to the large value of J, the outer lines of the AB patterns are expected to be very weak and could not be detected at either X-band or Q-band. The large value of J also caused difficulties with the perturbation calculation of the spectra at X-band[2,8] so the values of J for this compound were based on simulations at Q-band.

The values of J for the $VO(tfac)_2$ and $VO(hfac)_2$ adducts with ligands I–XI are summarized in Table I. Since the values of J in toluene, CH_2Cl_2, $CHCl_3$, and mixtures of these solvents differed by less than 10%, the values in Table I are the averages of the values obtained in several of these solvents. The low solubility of some of the ligands in toluene prevented the obtaining of spectra of some of the adducts in toluene solution.

Spectra of some of the adducts were examined as a function of temperature, and the results are summarized in Table II. For the vanadyl complexes examined, the value of J changed by less than 15% between 20 and −40 °C. The small temperature dependence of J indicates that whatever temperature-dependent conformational equilibria exist for the ligands and their vanadyl complexes in this temperature range have little impact on the metal–nitroxyl interaction. This behavior is quite different from that of some of the copper complexes discussed below.

EPR Spectra of the Copper Complexes. Interpretation of the EPR spectra of the $Cu(hfac)_2$ adducts of ligands I–IV have been reported.[12,13] The EPR spectra of the adducts with ligands V–XI were analyzed analogously. The average values

Table I. Electron–Electron Coupling Constants at Room Temperature

L	$VO(tfac)_2$·L	$VO(hfac)_2$·L	$Cu(hfac)_2$·L
I	1800[b]	2000[b]	620[c]
II	430	430	490[c]
III	{110 130	118	44[d]
IV	34	36	{37[d] 94
V	{400 475	375	160
VI	94	95	60
VII	{375 445	420	160
VIII	{105 118	124	32
IX	160	180	4
X	7	7	<2
XI	{130 160	154	47

[a] Values are given in gauss for spectra at X-band unless otherwise noted. The values are the averages of those observed for spectra taken in several of the following solvents: toluene, CCl_4, CH_2Cl_2, C_2HCl_3, or mixtures of these solvents. [b] On the basis of spectra taken at Q-band. [c] Value taken from ref 13. [d] Value taken from ref 12.

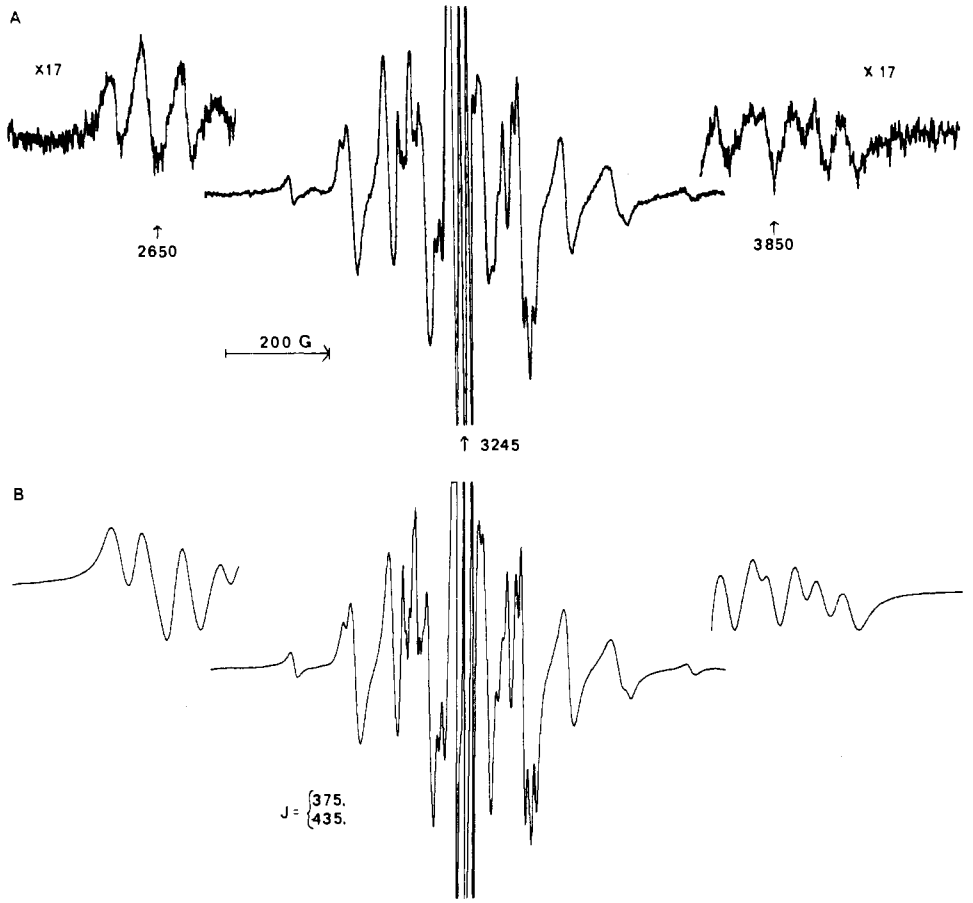

Figure 3. X-band EPR spectra of $VO(tfac)_2$·VII in CH_2Cl_2 solution at room temperature. (A) 1000-G scan of the inner lines of the AB pattern obtained with 60-mW power and 0.63-G modulation amplitude. The inserts show the metal outer lines of the AB pattern and were obtained with the product of modulation amplitude, gain, and square root of power 17 times greater than for the central portion of the spectrum. (B) Computer-simulated spectrum obtained with equal populations of two species with J = 375 and 435 G.

Table II. Temperature Dependence of Electron–Electron Coupling Constants, J[a]

complex	solvent	J at room temp[b]	J at lower temp[c]
$VO(tfac)_2$·III	$CHCl_3$	115, 135	130, 150 (−40)
$VO(tfac)_2$·IV	$CHCl_3$	35	40 (−40)
$VO(tfac)_2$·VI	$CHCl_3$	90	85 (−40)
$VO(tfac)_2$·IX	$CHCl_3$	160	140 (−30)
$Cu(hfac)_2$·I	toluene	615	470 (−70)
$Cu(hfac)_2$·II	toluene	490	320, 500 (−70)
$Cu(hfac)_2$·III	toluene	44	62 (−60)[d]
$Cu(hfac)_2$·IV	toluene	37, 94	37, 125 (−60)[d]
$Cu(hfac)_2$·V	2:1 C_2HCl_3/toluene	180	175 (−25)
$Cu(hfac)_2$·VI	2:1 C_2HCl_3/toluene	80	180 (−25)
$Cu(hfac)_2$·VII	2:1 C_2HCl_3/toluene	160	175 (−20)
$Cu(hfac)_2$·VIII	2:1 C_2HCl_3/toluene	23	48 (−20)
$Cu(hfac)_2$·IX	2:1 C_2HCl_3/toluene	7	48 (−60)

[a] Values of J in gauss for spectra taken at X-band. [b] 20–22 °C. [c] The low-temperature values were obtained at different temperatures determined by the solubilities of the compounds. The temperature (°C) at which each value was obtained is given in parentheses. [d] Value taken from ref 12.

of J obtained in several solvents are reported in Table I.

The temperature dependence of the values of J obtained for the $Cu(hfac)_2$ adducts of ligands I–IX is summarized in Table II. In general the values of J for the $Cu(hfac)_2$ adducts are more strongly temperature dependent than for the analogous $VO(tfac)_2$ adducts with the same ligands. The differences in the temperature dependence of J may result from a greater ease of geometrical distortion for the 5-coordinate copper complexes than for the 6-coordinate vanadyl complexes. In ligands II, IV, VI, and VIII the spin label is attached to the 3-position of the pyridine ring. For $Cu(hfac)_2$·IV two isomers with different values of J were observed in toluene solution at 20 and −70 °C. For $Cu(hfac)_2$·II a single value of J was observed at 20 °C but below −30 °C two isomers with different values of J were observed in the EPR spectra. Analysis of the temperature dependence of the relative populations and of the values of J indicates that the spectrum observed at room temperature is an average of the spectra for the two low-temperature isomers. Thus it appears that although both $Cu(hfac)_2$·II and $Cu(hfac)_2$·IV exist as two isomers, the rate of interconversion of the two species is fast on the EPR time scale at room temperature for $Cu(hfac)_2$·II and slow for $Cu(hfac)_2$·IV. The low solubilities of $Cu(hfac)_2$·VI and $Cu(hfac)_2$·VIII precluded studies below −20 °C. However, for both complexes, the value of J in toluene solution more than doubled between 20 and −20 °C. Such a large temperature dependence of J indicates substantial conformational changes within this temperature range. A possible explanation is that two isomers with temperature-dependent populations and values of J are rapidly interconverting on the EPR time scale as was observed for $Cu(hfac)_2$·II in this temperature interval. Proposed geometries for these isomers are discussed below.

Geometry of the Vanadyl Complexes. The coordination of a series of 4-substituted pyridines to $VO(acac)_2$ was studied by Caira et al.[18] Based on changes in the V=O stretch in the IR spectrum, they concluded that coordination of the pyridine occurred either cis or trans to the V=O bond and that subtle factors controlled the equilibrium.[18] Al-Niami et al. studied the coordination of 4-methylpyridine *N*-oxide to a series of vanadyl β-diketonates including $VO(acac)_2$ and

(18) Caira, M. R.; Haigh, J. M.; Nasimbeni, L. R. *J. Inorg. Nucl. Chem.* **1972**, *34*, 3171–6.

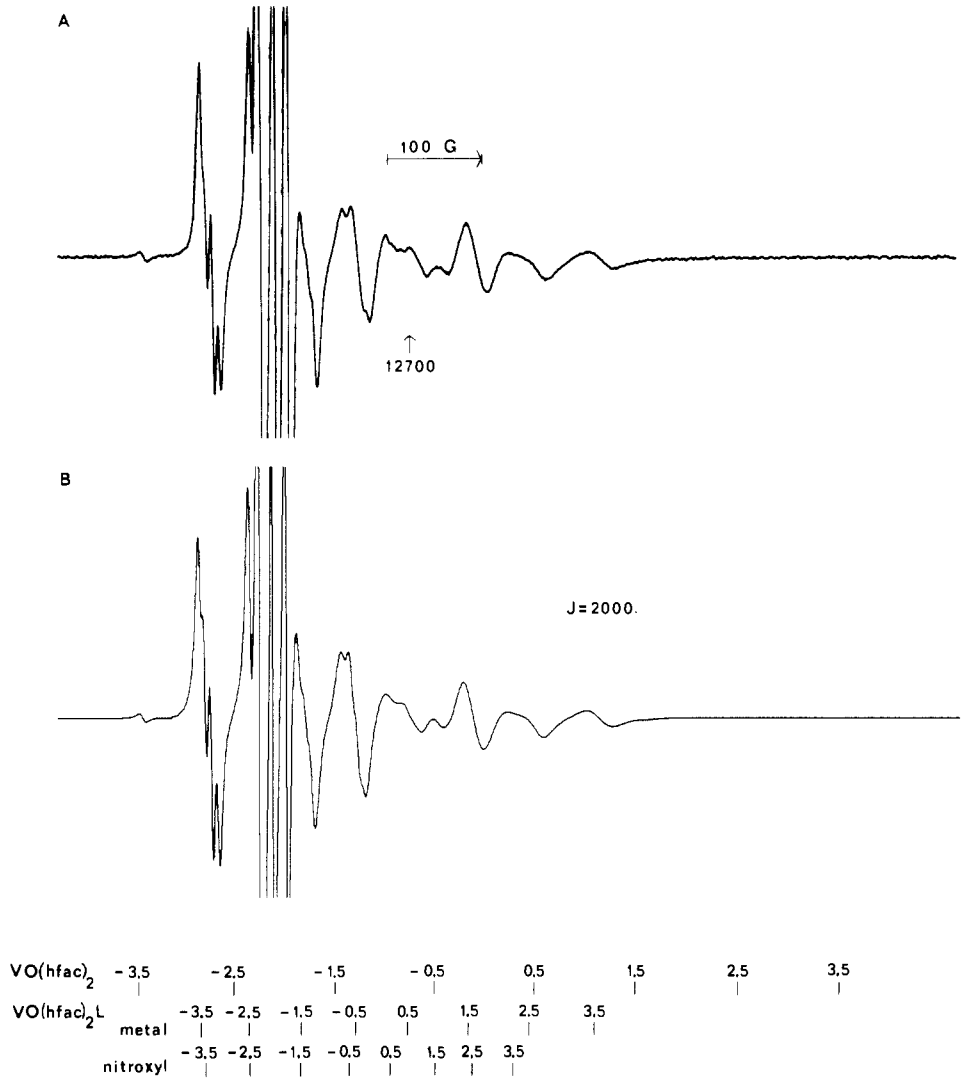

Figure 4. Q-band EPR spectra of $VO(hfac)_2$·I in CH_2Cl_2 solution at room temperature. (A) 1000-G scan obtained with 37 mW power and 0.8-G modulation amplitude. (B) Computer-simulated spectrum obtained with J = 2000 G. The assignments of the lines are given below the spectrum.

$VO(tfac)_2$.[19] They observed that as the donor ability of the β-diketonate decreased there was an increasing tendency for the 4-methylpyridine *N*-oxide to coordinate cis to the V=O bond.[19] For the $VO(acac)_2$ adduct there was a mixture of cis and trans isomers with a preference for the trans isomer, but for $VO(tfac)_2$ they observed only the cis isomer.[19] On the basis of these results, it seems likely that for the pyridine ligands studied here, $VO(tfac)_2$·L and $VO(hfac)_2$·L, would exist predominantly as the cis isomers. IR spectra of $VO(tfac)_2$·L (L = I–XI) in CH_2Cl_2 showed a single $\nu_{V=O}$ at 965 ± 3 cm^{-1}. This stretching frequency is in good agreement with the value of 968 cm^{-1} reported for $VO(tfac)_2$(4-methylpyridine *N*-oxide) which occurs as the cis isomer.[19] However, the IR bands for $\nu_{V=O}$ in $VO(tfac)_2$·L were sufficiently broad that the presence of a second isomer could not be ruled out. Similarly the IR spectra of $VO(hfac)_2$·L in CH_2Cl_2 had a single broad V=O stretch at 980 ± 5 cm^{-1}.

In the EPR spectra of five of the complexes, $VO(tfac)_2$·L (L = I–XI) two isomers were observed with values of J that differed by 12%–23%. In the other six cases, the lines were sufficiently broad that two values of J differing by up to 15% would not have led to resolved lines in the spectra. For all of the $VO(hfac)_2$·L (L = I–XI) complexes, a single isomer was observed in the EPR spectra. As discussed below, if the two isomers of $VO(tfac)_2$·L were due to coordination of the pyridine cis and trans to the V=O bond, then the resulting values of J for the two isomers would be expected to differ by much more than 12% to 23%. It seems more reasonable to attribute the two values of J to isomers XII and XIII both of which have L cis to the V=O bond. Since the CF_3C=O oxygen is a poorer donor than the CH_3C=O oxygen, it would be more readily displaced from the equatorial plane. The pyridine ligand could then bind trans to a CF_3C=O oxygen (XII) or trans to a CH_3C=O oxygen (XIII). This type of isomerism would not exist for $VO(hfac)_2$·L, consistent with the observation of a single isomer for all of the $VO(hfac)_2$ adducts.

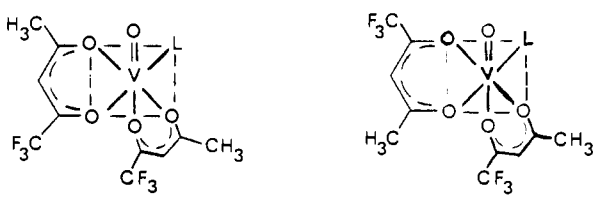

XII XIII

Geometry of the Copper Complexes. The frozen-solution EPR spectra of $Cu(hfac)_2$·py and of $Cu(hfac)_2$ adducts of diamagnetic analogues of ligands I–IV give values of $g_\parallel$, $g_\perp$, and $A_\parallel$ that are similar to values observed for square-pyramidal

(19) Al-Niami, N. S.; Al-Karaghouli, A. R.; Aliwi, S. M.; Jalhoom, M. G. *J. Inorg. Nucl. Chem.* **1974**, *36*, 283–8.

copper complexes.[12] These values, however, do not preclude some distortion from coplanarity of the four basal ligands. The large nitrogen hyperfine splitting (ca. 10 G[12]) due to interaction of the pyridine nitrogen with the copper unpaired electron suggests that the pyridine ligand is coordinated in the equatorial plane of the square pyramid.[20] In the crystal structure of $Cu(acac)_2$(4-aminopyridine), the pyridine coordinates in the equatorial plane of a square pyramid with the plane of the pyridine ring approximately perpendicular to the CuO_3N equatorial plane.[21] If the $Cu(hfac)_2$·L adducts adopt a similar geometry, then two isomers, XIV and XV, could exist for the

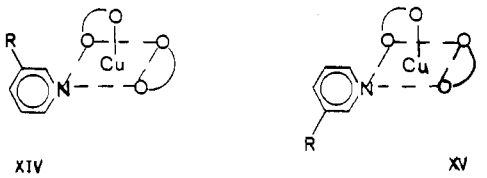

XIV XV

ligands that are spin labeled on the 3-position of the pyridine ring. The 3-substituent could be toward the axial oxygen (XIV) or toward the open face of the square pyramid (XV). This isomerism would not exist for the 4-substituted ligands, which is consistent with the observation of two isomers for some of the 3-substituted ligands but only one isomer for the 4-substituted ligands. Steric interaction between the bulky R groups and the acetylacetonate ring in XIV would be expected to cause a greater displacement of the pyridine below the equatorial plane of XIV than in XV, which could result in significantly different values of J for the two isomers. Thus all of the data for $Cu(hfac)_2$·L appear to be consistent with coordination of the pyridine ligands in the basal plane of an approximately square-pyramidal complex.

Mechanism of Electron Delocalization into the Pyridine Orbital. When an electron is added to the pyridine π^* LUMO to form the pyridine anion radical, the ratio of the spin density at the 4-position to the spin density at the 3-position of the pyridine ring is about 12.[22] NMR studies of pyridine coordinated to $Ni(acac)_2$, $Co(acac)_2$, and related compounds have observed that the ratio of the spin density at the 4-position to the spin density at the 3-position of the pyridine ring is in the range 0.25–0.30.[23-25] In these pyridine complexes the spin delocalization is primarily via σ bonding.[23-25] Comparison of the vanadyl complexes of ligands I–VIII indicates that the values of J for the 4-substituted ligands are 3.2–4.5 times larger than for the analogous 3-substituted ligands. Since the values of J for the vanadyl complexes are not strongly temperature dependent, the ratios do not vary significantly with temperature. For the copper complexes the comparison is more difficult because of the presence of isomers for the complexes of the 3-substituted ligands and the substantial temperature dependence of the values of J. If, as discussed above, the temperature dependence of J is due to changing populations of isomers with different values of J, then at lower temperatures the observed values of J would have greater contributions from the low-energy conformations of the molecules than at higher temperatures. Thus the comparisons for the copper complexes of ligands I–VIII are done at the lowest temperatures for which data are available. As discussed below, spin delocalization into the pyridine orbitals would be expected to decrease when the pyridine is distorted away from the basal plane of the square pyramid. Thus the value of J would be expected to be larger for isomer XV than for isomer XIV. For the 3-substituted ligands, the geometry of isomer XV would be expected to be more like the geometry of the $Cu(hfac)_2$ adducts of the 4-substituted ligands than would the geometry of isomer XIV. It therefore seems reasonable to compare the values of J for the 4-substituted ligands with the larger of the two values of J observed for the 3-substituted ligands. For ligands I–VI this ratio is between about 0.5 and 1.0. These results for the 3- and 4-substituted ligands suggest that π bonding plays a larger role than σ bonding in the spin delocalization from vanadyl to pyridine but that σ bonding dominates the spin delocalization from copper to pyridine. However, it is clear that there is extensive σ–π interaction in both cases. The observation that the nitrogen hyperfine splitting on the metal EPR signals for $M(hfac)_2$·py is larger for $M = Cu^{2+}$ ($A_N \approx 10$ G) than for $M = VO^{2+}$ ($A_N < 2$ G) is also consistent with a larger σ-bonding contribution to spin delocalization in $Cu(hfac)_2$·L than in $VO(hfac)_2$·L.

The ratio of the values of J for $Cu(hfac)_2$·VII and $Cu(hfac)_2$·VIII at −20 °C is 3.6, which is substantially larger than for the other pairs of $Cu(hfac)_2$ adducts of 4- and 3-substituted ligands. It is also surprising that the value of J for $Cu(hfac)_2$·VIII is only about 25% of the value of J for $Cu(hfac)_2$·VI at −20 °C since in all the other adducts examined for both copper and vanadyl the values of J are only slightly changed when a five-membered unsaturated nitroxyl ring is replaced by a six-membered unsaturated nitroxyl ring. The reason for the anomalous behavior of $Cu(hfac)_2$·VIII is not obvious, but it is possible that π interaction could be more important in these complexes than in other copper complexes.

If the z axis is defined to fall along the V=O bond and the x and y axes coincide with the V—O bonds, then the unpaired electron in $VO(acac)_2$ is in the d_{xy} orbital.[26] If the pyridine ligands coordinate cis to the V=O bond with the pyridine ring plane parallel to the z axis of the complex, then the geometry would be correct for π back-bonding from the vanadyl d_{xy} orbital to the pyridine π^* LUMO. However, if the pyridine ligands coordinate trans to the V=O bond, no π interaction with the unpaired electron would be expected. Thus the pattern of spin delocalization in the $VO(tfac)_2$·L and $VO(hfac)_2$·L complexes supports the proposal above that the ligands coordinate cis to the V=O bond.

With the use of an axis system analogous to that defined for $VO(acac)_2$·py, the unpaired electron in square-pyramidal copper(II) complexes is in the $d_{x^2-y^2}$ orbital.[20] Coordination of the pyridine ligands in the basal plane of the square pyramid would optimize the σ-bonding interaction between the unpaired metal electron and the pyridine ligand. Distortion of the pyridine ligand out of the basal plane would decrease the interaction with $d_{x^2-y^2}$ and would be expected to cause a decrease in the value of J.

As a result of the differences in spin delocalization mechanisms, when a 4-substituted pyridine ligand coordinates to $VO(tfac)_2$ or $VO(hfac)_2$ the value of J is about 3 times as large as when the same ligand is coordinated to $Cu(hfac)_2$. At room temperature ligand IX, which contains a pyrrolidine nitroxyl ring, is an exception to this pattern. The ratio of the values of J for the vanadyl and copper adducts is about 40. However, the value of J for $Cu(hfac)_2$·IX is unusually temperature dependent, increasing from about 4 G at room temperature to 48 G at −60 °C in 2:1 C_2HCl_3/toluene solution.

The value of J for $VO(tfac)_2$·IX decreases slightly over the same temperature interval, and at −60 °C the ratio of the values of J for the vanadyl and copper adducts of IX is about 3 as was observed for the other ligands at room temperature.

(20) McMillin, D. R.; Drago, R. S.; Nusj, J. A. *J. Am. Chem. Soc.* **1976**, *98*, 3120–6.
(21) Bushnell, G. W. *Can. J. Chem.* **1971**, *49*, 555–61.
(22) Myers, R. L.; Talcott, C. L. *Mol. Phys.* **1967**, *12*, 549–67.
(23) Happe, J. A.; Ward, R. L. *J. Chem. Phys.* **1963**, *39*, 1211–8.
(24) Holm, R. H.; Everett, G. W.; Horrocks, W. DeW. *J. Am. Chem. Soc.* **1966**, *88*, 1071–3.
(25) Maitani, T.; Chikuma, M.; Araishi, K.; Tanaka, H. *J. Inorg. Nucl. Chem.* **1979**, *41*, 1697–1702.
(26) Selbin, J.; Maus, G.; Johnson, D. L. *J. Inorg. Nucl. Chem.* **1967**, *29*, 1735–44.

In another spin-labeled copper complex containing a pyrrolidine nitroxyl, the value of J decreased rapidly as the temperature was increased from 20 to 100 °C.[4] One interpretation of this temperature data is that exchange interactions involving pyrrolidine rings are strongly dependent on the conformation of the pyrrolidine ring and that the barrier for the conformational changes varies considerably between derivatives.

Comparison of the Pyridine–Nitroxyl Linkages. The values of J for the complexes of ligands VII (amide) and XI (ester) indicate that the electron–electron interaction is about 3 times larger through the amide linkage than through the ester linkage. Comparison of the complexes of ligands III (Schiff base) and X (ester) shows that exchange is about 20 times larger for the Schiff base linkage than for the ester linkage. Ligands I (Schiff base) and IX (amide) show that exchange is about 10 times larger for the Schiff base linkage than for the amide linkage. The order ester < amide < Schiff base parallels the order of increasing double-bond character[27] between the carbon and the oxygen or nitrogen connecting the pyridine ring to the nitroxyl ring. Thus for both the copper and vanadyl adducts it appears that the interaction through the pyridine–nitroxyl linkage is dominated by π delocalization.

Comparison of the Nitroxyl Rings. The values of J for ligands V–VIII indicate that the exchange interactions are about the same for the unsaturated nitroxyl rings XVI and XVII except for the one case noted above. Comparison of

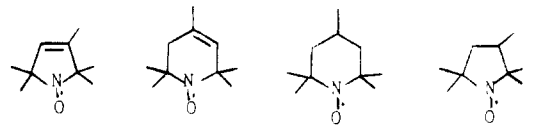

XVI XVII XVIII XIX

ligands I–IV indicates that interaction is about 15 times larger for the five-membered ring XIX than for six-membered ring XVIII. Comparison of ligands X and XI suggests that interaction is about 20 times larger for the unsaturated six-membered ring XVII than for the saturated six-membered ring XVIII. The data for ligands V and IX show that exchange is about twice as large for the unsaturated five-membered ring XVI as for the saturated five-membered ring XIX. Thus the combined data support the order XVIII < XIX < XVII ~ XVI.

Crystallographic studies of compounds containing nitroxyl rings provide possible clues to the origins of the differences between the nitroxyl rings. The details of four crystal structures have been reported which include the unsaturated five-membered ring XVI.[28-31] In each case the nitroxyl ring was found to be planar.[28-31] Two crystal structures of compounds containing the unsaturated six-membered ring XVII have shown that five of the ring atoms, including the nitroxyl nitrogen and the double-bonded carbons, are close to planar and one dimethyl carbon is displaced from the plane of the other atoms.[30,32] Thus in both of these rings the p–π orbital of the nitroxyl nitrogen is parallel to the p–π orbitals of the carbons on the double bond. π spin density transmitted through the pyridine–nitroxyl ring linkage and into the π orbitals of the double bond in the ring is thus in orbitals which are optimally oriented for direct interaction with the nitroxyl spin density in the nitrogen p orbital. The large values of J observed for ligands containing rings XVI and XVII are consistent with this geometry.

Crystal structures of the saturated six-membered ring XVIII have shown that it adopts a flattened chair conformation.[33-35] With this geometry there is no obvious pathway for direct interaction between π-spin density in the pyridine–nitroxyl ring linkage and spin density on the nitroxyl nitrogen. Interaction presumably occurs through the σ-bonding framework which would be expected to give a substantially smaller value of J for ligands containing ring XVIII than for XVI or XVII.

Ring XIX adopts a half-chair conformation in the compounds for which crystallographic data are available.[36,37] In this conformation there is the possibility of through-space interaction between unpaired spin density in the lone pair on the Schiff base or on the amide proton and the p–π orbital on the nitroxyl nitrogen which could result in stronger spin–spin coupling than through the σ bonds. Such an interaction would be strongly dependent on the conformation of the ring, consistent with the observations discussed above that in some cases the metal–nitroxyl interactions in compounds containing ring XIX are strongly temperature dependent.

The electron-spin delocalization pathways have been described in this paper in terms of σ and π orbitals and spin polarization, roughly in accord with the descriptions in chapter 6 of ref 38. It is recognized that more sophisticated treatments of electron correlation could yield different descriptions of the pathway.

Independent verification of some of the postulated isomers may not be possible. It is conceivable that the two "isomers" observed in some of the EPR spectra could be species which differ primarily in the way they are solvated or could be conformations stabilized by specific solvation. The postulates in this paper are based on consideration of potential barriers suggested by inspection of CPK molecular models and analogy with known crystal structures, coupled with the simplified σ, π interaction pathway model described above. That is, the picture of metal–nitroxyl interaction given is chemically reasonable but not proven.

Conclusions

Metal–nitroxyl interactions are sufficiently sensitive to the details of molecular geometry to provide a powerful probe of isomerism and conformational changes. Since these effects are difficult to probe by other techniques, the structural differences proposed in this paper are not readily verified. Further studies are in progress to determine whether results from related systems give analogous results.

Acknowledgment. This work was supported in part by the National Institutes of Health (GM21156). B.M.S. thanks Shivaji University (India) for a study leave.

Registry No. V, 79991-39-2; VI, 79991-40-5; VII, 79991-41-6; VIII, 79991-42-7; IX, 69432-68-4; X, 79991-43-8; XI, 79991-44-9; $VO(tfac)_2$·I, 79992-16-8; $VO(hfac)_2$·I, 79992-17-9; $VO(tfac)_2$·II, 79992-18-0; $VO(hfac)_2$·II, 79992-19-1; $VO(tfac)_2$·III, 79992-20-4; $VO(hfac)_2$·III, 79992-21-5; $VO(tfac)_2$·IV, 79992-22-6; $VO(hfac)_2$·IV, 79992-23-7; $Cu(hfac)_2$·IV, 72057-28-4; $VO(tfac)_2$·V, 79992-24-8; $VO(hfac)_2$·V, 79992-25-9; $Cu(hfac)_2$·V, 79992-26-0; $VO(tfac)_2$·VI,

(27) March, J. "Advanced Organic Chemistry: Reactions, Mechanisms, and Structure", 2nd ed.; McGraw-Hill: New York, 1977; Chapter 4.
(28) Boeyens, J. C. A.; Krueger, G. J. *Acta Crystallogr., Sect. B* **1970**, *B26*, 668–72.
(29) Turley, W.; Boer, F. P. *Acta Crystallogr., Sect. B* **1972**, *B28*, 1641–4.
(30) Alcock, N. W.; Golding, B. T.; Ioannou, P. V.; Sawyer, J. F. *Tetrahedron* **1977**, *33*, 2969–80.
(31) Bordeaux, D.; d'Assenza, G. *Cryst. Struct. Commun.* **1978**, *7*, 409–12.
(32) Shibaeva, R. P.; Rosenberg, L. P. *Zh. Struct. Khim.* **1975**, *16*, 258–61.
(33) Shibaeva, R. P. *Zh. Struct. Khim.* **1975**, *16*, 330–38 and references therein.
(34) McPhail, A. T.; Aboudonia, M. B.; Rosen, G. M. *Mol. Pharmacol.* **1976**, *12*, 590–7 and references therein.
(35) Guseinova, M. K.; Mamedov, S. D. *Zh. Struct. Khim.* **1978**, *19*, 702–10 and references therein.
(36) Chion, B.; Lajzerowicz, J. *Cryst. Struct. Commun.* **1978**, *7*, 395–8. Chion, B., Lajzerowicz, J.; Bordeaux, D.; Collet, A.; Jacques, J. *J. Phys. Chem.* **1978**, *82*, 2682–8 and references therein.
(37) Guseinova, M. K.; Mamedov, S. D.; Amiraslanov, J. R.; Kutovaga, T. M. *Zh. Strukt. Khim.* **1978**, *19*, 97–101 and references therein.
(38) Carrington, A.; McLachlan, A. D. "Introduction to Magnetic Resonance"; Harper and Row: New York, 1967.

79992-27-1; $VO(hfac)_2$·VI, 79992-28-2; $Cu(hfac)_2$·VI, 79992-29-3; $VO(tfac)_2$·VII, 79992-30-6; $VO(hfac)_2$·VII, 79992-31-7; $Cu(hfac)_2$·VII, 79992-32-8; $VO(tfac)_2$·VIII, 80010-10-2; $VO(hfac)_2$·VIII, 79992-33-9; $Cu(hfac)_2$·VIII, 79992-34-0; $VO(tfac)_2$·IX, 79992-35-1; $VO(hfac)_2$·IX, 79992-36-2; $Cu(hfac)_2$·IX, 79992-37-3; $VO(tfac)_2$·X, 79992-38-4; $VO(hfac)_2$·X, 79992-39-5; $Cu(hfac)_2$·X, 79992-40-8; $VO(tfac)_2$·XI, 79992-41-9; $VO(hfac)_2$·XI, 79992-42-0; $Cu(hfac)_2$·XI, 79992-43-1; 2,2,5,5-tetramethyl-1-oxypyrrolinyl-3-carboxylic acid chloride, 13810-21-4; 2,2,6,6-tetramethyl-1-oxy-1,2,5,6-tetrahydropyridinyl-4-carboxylic acid chloride, 79991-45-0; 2,2,5,5-tetramethyl-1-oxypyrrolidinyl-3-carboxylic acid chloride, 61593-19-9; 4-hydroxy-2,2,6,6-tetramethyl-1-oxypiperidine, 2226-96-2; 4-aminopyridine, 504-24-5; 3-aminopyridine, 462-08-8; isonicotinic acid, 55-22-1; 4-hydroxypyridine, 5382-16-1.

Contribution from the Institut für Anorganische, Analytische und Physikalische Chemie, Universität Bern, CH-3012 Bern, Switzerland

Optical Spectroscopy of $[(NH_3)_4Cr(OH)_2Cr(NH_3)_4]^{4+}$ and $[(en)_2Cr(OH)_2Cr(en)_2]^{4+}$

SILVIO DECURTINS, HANS U. GÜDEL,* and ANDREAS PFEUTI

Received March 18, 1981

The compounds $[(en)_2Cr(OH)_2Cr(en)_2]Cl_4·2H_2O$, $[(en)_2Cr(OH)_2Cr(en)_2]Br_4·2H_2O$, $[(NH_3)_4Cr(OH)_2Cr(NH_3)_4]Cl_4·4H_2O$, and $[(NH_3)_4Cr(OH)_2Cr(NH_3)_4]Br_4·4H_2O$ were prepared, structurally characterized, and studied by optical single-crystal absorption spectroscopy. Common to all the compounds is a strong linear dichroism. This is the result of unusually intense spin-allowed d–d transitions polarized perpendicular to the I plane. This behavior is rationalized in terms of an intensity stealing mechanism from ligand $\rightarrow e_g$ charge-transfer transitions. The exchange coupling is antiferromagnetic with parameters $2J$ on the order -1 cm^{-1} in the $[NH_3]$ compounds and -31 and -30 cm^{-1} in $[en]Cl_4·2H_2O$ and $[en]Br_4·2H_2O$, respectively. These differences in magnetic properties are accompanied by differences in the spectroscopic behavior, and they have a common physical origin. In the [en] compounds the hydrogen atom lies more or less in the plane defined by I, while in the $[NH_3]$ salts it is forced out of this plane by hydrogen bonding. The p_x orbital (x is perpendicular to I) on the bridging oxygen is fully available for π bonding to the chromium in the [en] compounds, while in the $[NH_3]$ compounds it is not. The superexchange pathway through $p_x(O)$ is thus blocked to a large extent in $[NH_3]Cl_4·4H_2O$ and $[NH_3]Br_4·4H_2O$, and the ligand field felt by chromium is sufficiently altered to produce significant changes in the optical spectra.

Introduction

Structural and magnetochemical properties of di-μ-hydroxo-bridged chromium(III) species are being intensively studied at present.[1-4] One of the main aims is to establish a correlation between structural properties and the magnitude of the exchange splitting of the ground state. Pedersen and co-workers were the first to point to the importance of the position of the hydrogen atom in these structural–magnetic correlations.[1] Several examples of both dinuclear and tetranuclear complexes exhibiting di-μ-hydroxo bridging show that a correlation exists between the magnitude of the exchange parameter and the displacement of the hydrogen atom out of the

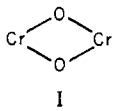

I

plane.[4,5] If the main superexchange pathway is through π bonding via the p_x orbital (coordinate system Figure 1) at the oxygen, such a correlation is most easily understood.

An analysis of electronically excited ^2E states, from which, at least in principle, the dominant contributions to the net exchange can be deduced, has not been done for di-μ-hydroxo-bridged chromium(III) species. In a systematic study of a large number of complexes by single-crystal absorption spectroscopy, we found that compounds containing $[(en)_2Cr(OH)_2Cr(en)_2]^{4+}$ (abbreviated [en] in the following) and $[(NH_3)_4Cr(OH)_2Cr(NH_3)_4]^{4+}$ (abbreviated $[NH_3]$) generally exhibited much more fine structure in the region of spin-forbidden transitions than any of the other complexes. Focusing our attention on [en] and $[NH_3]$ compounds, we found a new modification of $[NH_3]Cl_4·4H_2O$ and $[NH_3]Br_4·4H_2O$. In this modification, the antiferromagnetic coupling of the chromium(III) centers in the $[NH_3]$ complexes is very weak with $2J$ on the order of -1 cm^{-1}.[6] In the corresponding [en] compounds, on the other hand, the exchange coupling is stronger by more than 1 order of magnitude (Table I).[2] In their optical spectroscopic behavior, $[en]Cl_4·2H_2O$ and $[en]Br_4·2H_2O$ on the one hand and $[NH_3]Cl_4·4H_2O$ and $[NH_3]Br_4·4H_2O$ on the other show close similarities as well as marked differences. We decided to explore the physical origins of these interesting magnetic and spectroscopic phenomena in detail. In the present paper the general spectroscopic properties are discussed and related to structural and exchange effects.

Experimental Section

(1) Preparation, Structure, and Morphology. $[(en)_2Cr(OH)_2Cr(en)_2]Cl_4·2H_2O$ and $[(en)_2Cr(OH)_2Cr(en)_2]Br_4·2H_2O$. The compounds were prepared following literature procedures.[7] Single crystals large enough for optical and spectroscopic investigation were obtained by slow diffusion of the counterion through a dialyse membrane into a saturated solution of the complex. Shiny red-violet crystals with well-developed faces and edge lengths up to 0.5 mm were thus obtained. Both compounds are isomorphous and crystallize in the triclinic system, space group $P\bar{1}$. The grown crystal faces were found to be {100}, {010}, and {001} from Bürger precession X-ray photographs.

$[(NH_3)_4Cr(OH)_2Cr(NH_3)_4]Br_4·4H_2O$ was prepared following a literature method.[7]

$[(NH_3)_4Cr(OH)_2Cr(NH_3)_4]Cl_4·4H_2O$ was prepared from the perchlorate salt.[7] A 1.4-mmol sample of $[(NH_3)_4Cr(OH)_2Cr(NH_3)_4](ClO_4)_4·2H_2O$ is added to 5 mL of a saturated (at room tem-

(1) (a) Josephsen, J.; Pedersen, E. *Inorg. Chem.* **1977**, *16*, 2534. (b) Michelsen, K.; Pedersen, E. *Acta Chem. Scand., Ser. A* **1978**, *A32*, 847.
(2) Beutler, A.; Güdel, H. U.; Snellgrove, T. R.; Chapuis, G.; Schenk, K. *J. Chem. Soc., Dalton Trans.* **1979**, 983.
(3) Cline, S. J.; Kallesøe, S.; Pedersen, E.; Hodgson, D. J. *Inorg. Chem.* **1979**, *18*, 796.
(4) Pedersen, E., private communication.
(5) Güdel, H. U.; Hauser, U. *J. Solid State Chem.* **1980**, *35*, 230.
(6) Decurtins, S.; Güdel, H. U., to be submitted for publication.
(7) Springborg, J.; Schäffer, C. E. *Inorg. Synth.* **1978**, *18*, 75.

0020-1669/82/1321-1101$01.25/0